Comparison of Spiral Multidetector CT Angiography and Myocardial Perfusion Imaging in the Noninvasive Detection of Functionally Relevant Coronary Artery Lesions: First Clinical Experiences

Marcus Hacker, MD[1]; Tobias Jakobs, MD[2]; Florian Matthiesen[1]; Christian Vollmar, MD[3]; Konstantin Nikolaou, MD[2]; Christoph Becker, MD[2]; Andreas Knez, MD[4]; Thomas Pfluger, MD[1]; Maximilian Reiser, MD[2]; Klaus Hahn, MD[1]; and Reinhold Tiling, MD[1]

[1]Department of Nuclear Medicine, University of Munich, Munich, Germany; [2]Department of Radiology, University of Munich, Munich, Germany; [3]Department of Neurology, University of Munich, Munich, Germany; and [4]Department of Cardiology, University of Munich, Munich, Germany

Compared with conventional coronary angiography, spiral multidetector CT (MDCT) angiography has delivered promising accuracy in the detection and validation of coronary lesions. Myocardial perfusion imaging (MPI) using SPECT is an established method for noninvasively assessing the functional significance of coronary stenoses and delivers valuable information for risk stratification. This retrospective analysis compared the accuracies of MDCT angiography and MPI in the detection of hemodynamically relevant lesions of the coronary arteries. **Methods:** Twenty-five patients with suspected or known coronary artery disease were studied. Electrocardiographically gated MPI and 16-MDCT angiography were performed. Myocardial perfusion images were analyzed by 2 experienced observers, and reversible and fixed perfusion defects were detected and allocated to their corresponding coronary vessels. For the evaluation of MDCT angiography, image quality was determined, and lesions $\geq$ 50% and luminal narrowing $<$ 50% were visually assessed and characterized by 2 independent observers unaware of the results of MPI. **Results:** Ninety-nine coronary vessels were analyzed, and the quality of MDCT angiography images was assessed for 330 coronary segments. Coronary artery diameter was interpretable for 231 (70%) of 330 segments, whereas in 99 (30%) of 330 segments, vessel diameter could not be evaluated because of heavy calcifications, blurring, motion artifacts, or intracoronary stents. MDCT angiography detected stenoses $\geq$ 50% in 15 of 100 coronary arteries. Eight (53%) of 15 stenoses $\geq$ 50% showed reversible or fixed perfusion defects in the corresponding myocardial areas on MPI. Sensitivity, specificity, and negative and positive predictive values were 100%, 87%, 100%, and 29%, respectively, for the ability of MDCT angiography to detect reversible perfusion defects in the corresponding myocardial areas. **Conclusion:** MDCT angiography detected myocardial ischemia, as defined by reversible perfusion defects on MPI, with a positive predictive value of 29% in a nonselected study cohort. Compared with MPI alone, MDCT angiography added important morphologic information, but MPI remains mandatory for evaluating the functional relevance of coronary artery lesions.

Key Words: multidetector CT angiography; myocardial SPECT; coronary artery disease

J Nucl Med 2005; 46:1294–1300

Compared with conventional coronary angiography, spiral multidetector CT (MDCT) angiography has delivered promising accuracy in the detection and validation of coronary lesions. Moreover, the magnitude of coronary artery calcification can clearly be detected using CT techniques (*1–3*), and initial results also suggest that even preclinical atheroma and noncalcified plaque tissue, which may contribute to the development of acute coronary events (*4–9*), can be identified (*10–13*). Particularly, scanners with 16 or more slices and a faster rotation have been shown to reduce motion artifacts and partial-volume effects in cases of heavy calcifications, though both remain major limitations preventing the use of MDCT angiography in clinical routine (*14–20*). Myocardial perfusion imaging (MPI) using SPECT is an established method for noninvasively assessing the functional significance of coronary stenoses and delivers valuable information for risk stratification. Patients with stable angina and normal MPI results have a low risk of death or fatal myocardial infarction; therefore, no intervention is required for these patients (*21–24*). Even patients with angiographically documented coronary artery disease

Received Dec. 15, 2004; revision accepted May 9, 2005.

For correspondence or reprints contact: Marcus Hacker, MD, Klinik und Poliklinik für Nuklearmedizin der LMU, Ziemssenstrasse 1, 80336 München, Germany.

E-mail: marcus.hacker@med.uni-muenchen.de

(CAD) but normal MPI results have been shown to have similar low event rates (*25,26*). Furthermore, MPI identifies myocardial perfusion defects indicating the functional relevance of coronary artery stenoses and thus delivers important information for clinical decision making.

To date, no data have been published correlating MDCT angiography with MPI, both being methods with the potential to serve as noninvasive "gatekeepers" for the performance of conventional coronary angiography. This retrospective analysis compared the accuracies of MDCT angiography and MPI in the detection of perfusion defects referable to hemodynamically relevant coronary artery lesions. As such, this analysis may serve as a pilot study for the use of combined MDCT angiography and MPI for the noninvasive detection and classification of coronary artery lesions.

MATERIALS AND METHODS

Patient Selection

Twenty-five consecutive patients who had undergone MPI within 40 d of MDCT angiography were enrolled in this study; patients who had had a cardiac intervention within this period were excluded. The examinations were performed between February 2002 and August 2004 according to the following protocols.

Myocardial Scintigraphy

A same-day stress/rest electrocardiography-gated MPI protocol was performed on all patients, using weight-adjusted doses of 4 MBq/kg (at least 300 MBq of ^{99m}Tc-methoxyisobutylisonitrile) at peak ergometric or pharmacologic stress and 10 MBq/kg (at least 700 MBq) at rest at least 3 h after the first injection.

The ergometric stress test was performed on an electronically braked bicycle ergometer and was terminated according to standard criteria: reaching age-predicted submaximal heart rate (heart rate $\geq$ [220 $-$ age in years $\times$ 0.85]), severe chest pain, ST-segment depression $>$ 0.2 mV, severe cardiac arrhythmia, hypertension ($>$240/120 mm Hg), or a fall of $>$40 mm Hg in systolic blood pressure. Pharmacologic stress was obtained by administration of 0.56 mg of dipyridamole per kilogram of body weight over 5 min. If systolic blood pressure was $>$120 mm Hg, 0.8 mg of nitroglycerin was administered sublingually to the patients before injection of the radiopharmaceutical for the rest image.

Gated images were acquired on a triple-head camera system (Prism 3000 XP; Philips) using a low-energy, high-resolution, parallel-hole collimator with a 360° rotation in continuous mode. An electrocardiogram R-wave detector provided a gate to acquire 12 frames per cardiac cycle during the poststress and postrest acquisitions. The summed image set was normalized conventionally for comparison of stress and rest images. For each study, short and long axes were reconstructed. A standardized filter (low-pass fourth-power; cutoff frequency, 0.26) was used.

Scintigraphic stress and rest images were evaluated visually by 2 experienced observers, who reached a consensus on the findings. The observers were unaware of the findings of MDCT angiography but aware of the size, weight, and sex of the patients. Raw data cines, gated SPECT wall motion, and wall thickening were analyzed, and quantitative analysis software (Hermes Perfit; Nuclear Diagnostics) was used for defect detection and quality control. Perfusion defects were allocated to coronary arteries according to the coronary perfusion type of the subject as described previously (*27*). Defects in the anterior wall and septal region were allocated to the left anterior descending coronary artery (LAD); defects in the lateral wall, to the left circumflex coronary artery (LCX); and inferior defects, to the right coronary artery (RCA). Apical defects were considered to be in the LAD region, unless the defect extended to the lateral (LCX) or inferior (RCA) wall. In the watershed regions, the extension of a defect to the anterior, lateral, or inferior wall was decisive for the allocation of a coronary artery to the vascular bed. Furthermore, distinct defects affecting both the LAD region and the LCX region were rated as left main artery (LM) disease.

To ensure that reversible perfusion defects on MPI were true-positive findings, all patients underwent conventional coronary angiography and revascularization therapy in case of coronary artery stenosis.

Spiral MDCT Angiography

The MDCT angiography datasets were acquired using the 12 inner detectors of a 16-MDCT scanner (Sensation 16; Siemens Medical Solutions) and a previously described protocol (*15*).

In brief, a bolus of 120 mL of contrast agent (Solutrast 300, 300 mg/mL; Altana) was injected intravenously (5 mL/s). As soon as the signal density level in the ascending aorta reached a predefined threshold of 100 HU, the acquisition of the CT data and the electrocardiogram trace was started. Detector collimation was 12 $\times$ 0.75 mm; rotation time, 420 ms; and tube voltage, 120 kV at a current of 500 mAs during the diastolic phase of the cardiac cycle, and tube current was reduced by 80% during the remaining phase of the R-R interval, leading to an estimated mean effective radiation dose of approximately 4.3 mSv (*28*). Images were reconstructed with an acquisition time of 210 ms in diastole 350–450 ms before the R wave using retrospective electrocardiogram gating. Motion artifacts can be avoided only in the presence of a heart rate of $<$65 beats per minute (*29*); therefore, all patients with heart rates of $>$65 beats per minute were pretreated with 50–100 mg of oral metoprolol 1 h before the scan or intravenously with 10–20 mg of metoprolol directly before the scan. The voxel size of the resulting CT images was 0.6 $\times$ 0.6 $\times$ 1 mm.

The CT datasets were analyzed by 2 independent, experienced readers using a Leonardo workstation (Siemens), who reached a consensus on the findings. In a first step, image quality was determined by the investigators on the basis of the presence of motion artifacts and vessel calcifications. Image quality was graded as excellent (no motion artifacts present), good (minor motion artifacts present), moderate (substantial motion artifacts present, but luminal assessment of significant stenosis still possible), heavily calcified (vessel lumen obscured by calcification), or blurred (only contrast visualization inside the vessel possible; no luminal assessment of significant stenosis possible). Results were documented separately for all coronary segments using a modified American Heart Association classification as described recently by Kuettner et al. (*20*). Each bypass graft was counted as an additional segment. Sections containing an intracoronary stent could not be evaluated, but the stent location was noted. The observer subjectively identified a prior myocardial infarction by considering blockage of contrast material and decreased CT attenuation. The latter was seen with the help of CT density values (HU), which were measured for areas of suspected infarction and representative noninfarcted areas in the same patient, with standard-sized (1 cm^2), circular regions of interest placed over corresponding areas as

described previously (*30*). Suspected areas of myocardial infarction were allocated to respective coronary vessels as described for myocardial scintigraphy.

The readers visually estimated whether stenoses were ≥50% or <50% and allocated them to the LM, LAD, LCX, or RCA. Bypass grafts were rated as belonging to their respective coronary arteries. Lesion structure was stated as calcified, not calcified, or mixed when appropriate (*9*).

RESULTS

Twenty-five patients (15 men and 10 women; mean age ± SD, 63 ± 12.3 y; range, 29–84 y) were eligible to be included in the study. MDCT angiography was performed 13 ± 11 d before or after MPI for all patients. The study cohort consisted of 11 patients with suspected CAD and 14 patients with known CAD (Table 1). Overall, 99 coronary vessels were analyzed; in 1 patient the LM segment was not disposed as a normal variant.

Results of MDCT Angiography

Mean heart rate for MDCT angiography acquisition was 60 ± 10 beats per minute (range, 47–85 beats per minute). Image quality was assessed for 330 coronary segments on MDCT angiography (324 coronary artery segments and 6 bypass grafts). The number of segments classified as excellent, good, or moderate was 231 (70%). Twenty-three segments (7%) were rated as heavily calcified and 30 (9%) as blurred; 23 (7%) were not evaluable because of motion artifacts and 23 (7%) because of intracoronary stents. Thus, vessel diameter could not be evaluated for 99 (30%) of 330 segments.

MDCT angiography detected 47 stenoses in 44 of 99 coronary arteries. Stenoses were classified as ≥50% in 17 of 99 coronary arteries: 1 LM, 9 LAD, 3 LCX, and 4 RCA. Four patients showed myocardial areas with decreased CT attenuation suspected of representing prior myocardial infarction: 3 in the LAD and 1 in the territory supplying the RCA. In 1 of these 4 patients, additional blockage of contrast material was detected just posterior to a ≥50% stenosis in the middle segment of the RCA (Fig. 1). Stenoses were rated as <50% for 30 coronary arteries: 8 LM, 6 LAD, 5 LCX, and 11 RCA; 3 coronary arteries showed stenoses of both ≥50% and <50%. In 55 coronary arteries, no luminal narrowing could be detected, nor was luminal narrowing found in any of the 6 bypass grafts. Twenty of the 47 detected stenoses had plaque that was classified as calcified; 23, as mixed; and 4, as noncalcified.

TABLE 1
Patient Characteristics (n = 25)

Variable	Value
Sex (M/F)	17/8
Age (y)	63 ± 12
Body mass index	27 ± 4
Suspected CAD	11 (44)
Known CAD	14 (56)
1-vessel disease	4 (16)
2-vessel disease	5 (20)
3-vessel disease	4 (16)
4-vessel disease	1 (4)
Previous percutaneous transluminal coronary angioplasty or stenting	14 (56)
Bypass graft	3 (12)
Prior myocardial infarction	6 (24)
Diabetes mellitus	6 (24)
Hypertension	13 (52)
Hypercholesterolemia (>6.2 mmol/L)	14 (56)
Current smoker	9 (36)

Values are mean ± SD, or number with percentage in parentheses.

Results of MPI

Myocardial perfusion images could be analyzed for 25 of 25 patients. Five reversible and 6 fixed defects were detected in 10 of 25 patients, 1 of whom showed both reversible and fixed perfusion defects. Of the 5 reversible perfusion defects, 4 were in the LAD and 1 in the LCX, and of the 6 fixed defects, 3 were in the LAD, 2 in the RCA, and 1 in the LCX.

Comparison of MDCT Angiography and MPI

Eight (47%) of 17 stenoses ≥ 50% as detected by MDCT angiography showed perfusion defects in the corresponding myocardial area on MPI. Five of these perfusion defects were reversible and 3 were fixed. Blockage of contrast material was detected posterior to 1 of these 8 stenoses, as was CT attenuation in the corresponding myocardial area. MPI showed a fixed perfusion defect with residual ischemia (Fig. 1). One patient with stenosis ≥ 50% and without blockage of contrast material showed decreased CT attenuation in the supplied myocardial region. In 2 patients with suspected myocardial infarction, no stenosis ≥ 50% was found in the supplying coronary artery, but 1 of the 2 patients had an intracoronary stent.

Nine (53%) of 17 stenoses ≥ 50% showed no perfusion defects on MPI (Fig. 2). None of the stenoses < 50% as detected by MDCT angiography in 30 coronary arteries was associated with a perfusion defect.

Sensitivity, specificity, and negative and positive predictive values for MDCT angiography to detect reversible defects on MPI were 100%, 87%, 100%, and 29%, respectively, with an accuracy of 88%. When information from MDCT angiography about the myocardial infarction was added, specificity and positive predictive value increased to 89% and 33%, respectively.

Sensitivity, specificity, and negative and positive predictive values for MDCT angiography to detect any perfusion defect in the target area on MPI were 73%, 90%, 96%, and 47%, respectively. Accuracy was 88% (Table 2).

In 5 of 5 patients with reversible perfusion defects, the appropriate coronary artery stenosis could be detected on MDCT angiography. In 4 of 6 patients with fixed perfusion defects on MPI, CT attenuation was detected in the corre-

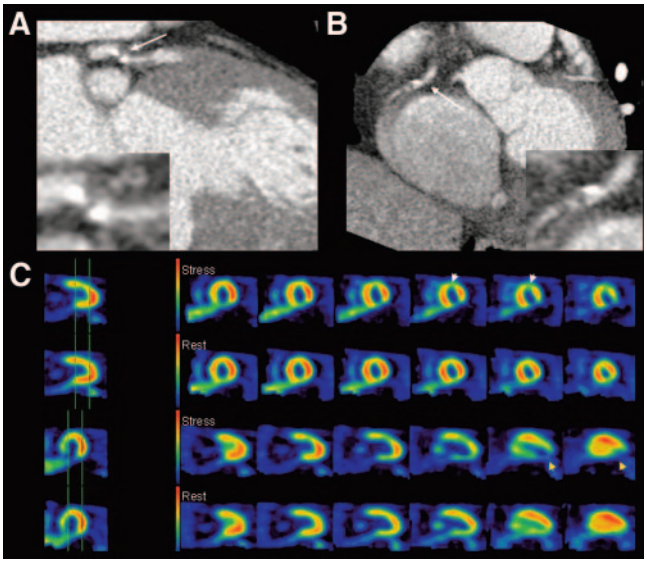

FIGURE 1. Patient with stenosis of LAD classified as ≥50% on MDCT angiography and associated with reversible perfusion defects in anterior wall. Blockage of contrast material posterior to stenosis of ≥50% was detected in RCA, and corresponding fixed perfusion defect with residual ischemia was found in posterior wall. (A) Maximum-intensity projection MDCT angiogram (left anterior oblique view) shows proximal LAD with partly calcified, reduced lumen (arrow). (B) Axial MDCT angiogram shows proximal RCA with partly calcified, reduced lumen (arrow). (C) Axial (top 2 rows) and sagittal (bottom 2 rows) MPI slices at stress and rest show reversible perfusion defects in anterior wall (white arrowheads) and fixed perfusion defects with residual ischemia in posterior wall (yellow arrowheads).

sponding myocardial area, but in only 3 of 6 patients could the appropriate lesions be found. In the remaining 3 of 6 patients, the appropriate lesions were not found because of heavy calcifications in 2 patients and an intracoronary stent in 1 patient. Generally, in cases of heavy calcifications or intracoronary stents, the readers were not able to grade the luminal narrowing as ≥50% or <50%, but the perfusion defects could be allocated to the appropriate lesions.

When we focused on the 15 patients without perfusion defects on MPI, MDCT angiography showed 5 stenoses ≥ 50% and 22 stenoses < 50% in 25 coronary arteries, and 15 calcified and 12 mixed plaques were registered. The locations of these stenoses and the consistency of the plaque are listed in Table 3. No relationship was found between plaque consistency and the appearance of perfusion defects.

DISCUSSION

The most important finding of this study was that MDCT angiography using a 16-MDCT scanner showed a low positive predictive value of 29% for identifying areas of ischemia in need of revascularization. Even when myocardial wall was evaluated in terms of suspected myocardial infarction, positive predictive value remained low, at 33%.

Promising results have been published for MDCT angiography in the detection of coronary artery lesions in patients with suspected CAD. Nieman et al. first reported a high overall sensitivity and specificity of 95% and 86%, respectively, for detecting significantly stenosed branches (≥50%) in 59 patients, including only side branches with a diameter ≥ 2.0 mm and excluding intraluminal coronary stents because of the known low interpretability (*15*). Ropers et al. investigated 77 patients and found a worse overall sensitivity of 73% for detecting >50% stenoses. When only evaluable arteries were used, sensitivity increased to 92% in that study, and specificity was 93% (*14*). Similar results were recently reported by Kuettner et al., who investigated 60 patients and found an overall sensitivity and specificity of 72% and 97%, respectively. When the investigators included only patients with an Agatston score equivalent of <1,000, sensitivity and specificity increased to 98% and 98%, respectively (*20*).

However, despite improved image quality with 16-MDCT angiography, severe calcifications and higher heart rates as well as intracoronary stents still limit the interpretability of contrast-enhanced visualization of coronary arteries. Consequently, a worse sensitivity of 37% but a high specificity of 99% were reported recently by Kuettner et al. for the ability of MDCT angiography to detect and classify coronary artery stenoses in patients with angiographically proven CAD, who frequently have a higher extent of coronary calcium than do patients investigated for exclusion of CAD (*31*). Only 57% of coronary artery segments could be judged in that study, a rate even lower than the 70% of interpretable segments in the present study.

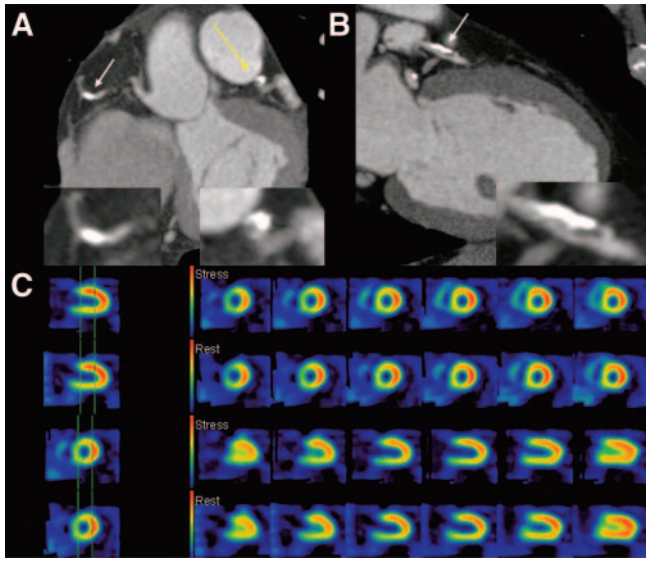

FIGURE 2. Patient with LAD stenosis of ≥50% and RCA stenosis of ≥50%, neither showing hemodynamic relevance on MPI. (A) Axial MDCT angiogram shows proximal RCA with calcified, reduced lumen (white arrow) and coronal view of mixed plaque in reduced lumen of LAD (yellow arrow). (B) Sagittal MDCT angiogram shows proximal LAD with partly calcified, reduced lumen (arrow). (C) Axial (top 2 rows) and sagittal (bottom 2 rows) MPI slices at stress and rest show homogeneous perfusion without perfusion defects.

TABLE 2
Accuracy of MDCT in Detecting Perfusion Defects in Target Area on MPI (n = 99 Coronary Arteries)

Parameter	Perfusion defect present	Perfusion defect not present	Sensitivity	Specificity	Negative predictive value	Positive predictive value	Accuracy
Any perfusion defect			0.73	0.90	0.96	0.47	0.88
Stenosis ≥ 50%	8	9					
No stenosis ≥ 50%	3	79					
Reversible perfusion defect			1.00	0.87	1.00	0.29	0.88
Stenosis ≥ 50%	5	12					
No stenosis ≥ 50%	0	82					

All these studies compared the morphologic accuracy of MDCT angiography with that of conventional coronary angiography. To date, no experience has been published on MDCT angiography in the detection of functionally relevant coronary artery lesions, even though the identification of coronary stenoses as functionally relevant has been shown to be a major prerequisite for clinical decision making (*32*). Thus, the present study retrospectively compared the results of MDCT angiography with those of MPI, which was used as the gold standard for the detection of perfusion defects in cases of hemodynamically relevant coronary artery stenoses. To avoid false-positive MPI results, we determined the correlation between reversible perfusion defects and conventional coronary angiography and, in 5 of 5 patients, found significant stenoses, all of which were eliminated during interventional therapy.

TABLE 3
Patients Without Perfusion Defect on MPI (n = 15)

Patient no.	Stenosis ≥ 50%				Stenosis < 50%
	LM	LAD	RCA	LCX	
1	—	—	—	—	3c
2	—	6c	—	—	5m, 11m, 12c
3	—	—	—	—	1m
4	—	—	—	—	6m
5	Not disposed as normal variant	6m	1c	—	1c, 11c
6	—	—	—	—	5m, 6m
7	—	—	—	—	1m, 5c
8	—	—	1m	—	—
9	—	—	—	—	1c, 5c
10	—	—	—	—	1c, 11c
11	—	—	—	—	5c, 6m
12	—	7m	—	—	10c, 11m
13	—	—	—	—	—
14	—	—	—	—	1c, 2c
15	—	—	—	—	—

c = calcified plaque; n = noncalcified plaque; m = mixed plaque.
Numbering scheme for coronary artery segments: 1 = proximal RCA; 2 = middle RCA; 3 = distal RCA; 4 = combined posterior descending and posterolateral branches of RCA; 5 = LM; 6 = proximal LAD; 7 = middle LAD; 8 = distal LAD; 9 = first diagonal LAD; 10 = second diagonal LAD; 11 = proximal LCX; 12 = distal LCX; 13 = first marginal branch of LCX.

Ninety-nine coronary vessels were investigated in 25 patients with suspected or known CAD, and MDCT angiography showed a high sensitivity of 100% for identifying coronary artery stenoses with a threshold value of 50% lumen narrowing leading to reversible perfusion defects on MPI. The sensitivity with 73% was weaker when MDCT angiography was compared with any perfusion defects detected by MPI, including fixed perfusion defects in cases of prior myocardial infarction. Less experience has been published on MDCT angiography in the detection of myocardial infarction, but it is supposed that both blockage of contrast material and the CT density values of myocardial areas can lead to the diagnosis of myocardial infarction, as was demonstrated by Nikolaou et al. (*30*). They reported an 85% sensitivity and 91% specificity for the ability of MDCT angiography to detect infarcted myocardial areas in 106 patients, 27 of whom had prior myocardial infarction. Applying these techniques for the identification of infarcted myocardial areas in the present study, we could detect the fixed perfusion defect of 4 of 6 patients on MPI. Two had stenoses ≥ 50% and 1 had blockage of contrast material, increasing both the specificity and the positive predictive value of MDCT angiography in the prediction of reversible perfusion defects on MPI and improving differentiation between ischemia and myocardial infarction.

Despite the low positive predictive value of MDCT angiography in the detection of hemodynamically relevant coronary artery lesions without preselection of patients, several arguments exist for performing MDCT angiography as a CAD diagnostic aid. Some investigators have suggested that future cardiac events may be predicted with the help of coronary calcium scores provided by MDCT angiography (*1,2,33*). Berman et al. recently demonstrated a potential role for applying coronary artery calcification screening after MPI among patients manifesting normal MPI results (*34*), a concept addressing the presence of subclinical atherosclerosis, which is hypothesized to affect the long-term risk of patients in different CAD risk groups. Pirich et al. recently reported that no significant correlation exists between calcium burden as measured by electron beam to-

mography and coronary flow reserve as quantified by ^{13}N-ammonia PET (*35*), leading to the conclusion that such vessel alterations cannot be detected by any form of stress testing, including MPI. In the present study, the 15 patients without perfusion defects on MPI showed 22 stenoses < 50% on MDCT angiography, consisting of 15 calcified and 12 mixed plaques, and no relationship was found between plaque consistency and the appearance of perfusion defects.

Furthermore, subclinical atherosclerosis might affect individual risk stratification and therapy, even if noncalcified plaque components are present (*4–9*). Leber et al. recently demonstrated, in 37 patients, that in cases of diagnostic image quality, MDCT angiography permits accurate identification of coronary plaque composition (*13*). Consequently, MDCT angiography has the potential to identify noncalcified or mixed plaques that are at increased risk for rupture leading to fatal cardiac events, especially those high-risk plaques that are missed by MPI screening because they do not lead to any perfusion defects. Thus, myocardial scintigraphy has been established as highly effective for risk stratification, particularly in patients with an intermediate or high likelihood of CAD, who are represented in the present study. Patients with normal MPI findings have a low risk for cardiac events during short-term follow-up (*36,37*).

Future investigations will have to clarify how subclinical atherosclerosis will affect both risk stratification and therapy planning, especially in patients with suspected CAD and no perfusion defects on MPI.

Besides detecting noncalcified or mixed plaques without hemodynamic relevance, MDCT angiography could add valuable information to MPI by allocating perfusion defects to specific epicardial coronary vessels—a well-known problem in nuclear cardiology (*38,39*). Future generations of MDCT angiography scanners with even more detector rows and decreased rotation times will provide improved spatial and temporal resolution and therefore might overcome the current major limitations of MDCT angiography—motion artifacts and impaired visualization of coronary segments that are heavily calcified or contain intraluminal stents. However, when segments or luminal diameters are not interpretable on MDCT angiography, the hemodynamic relevance of lesions can be determined when MPI information is considered. Further studies have to evaluate whether the combination of MPI and MDCT angiography with 2- or 3-dimensional image fusion using separate modalities or hybrid scanners (SPECT/CT) has potential to improve conventional allocation processes. Such a potential has already been demonstrated for the combination of conventional coronary angiography and MPI (*40–42*).

The present study had some limitations. It focused on the potential use of 16-MDCT angiography as a "gatekeeper" of invasive diagnostic and therapeutic procedures in patients with advanced coronary artery disease. Because, according to the current guidelines of the American College of Cardiology and the American Heart Association, the functional significance of coronary lesions as detected by myocardial scintigraphy or other noninvasive imaging modalities should be decisive for performing invasive diagnostic procedures or coronary interventions, conventional coronary angiography was deliberately not considered the gold standard. Because myocardial scintigraphy has shown high accuracy in the identification of hemodynamically significant coronary stenoses, and because MPI is most frequently used as the "gatekeeper" of invasive procedures for routine clinical diagnostics, 16-MDCT angiography was compared with MPI. The scintigraphic results in the case of reversible perfusion defects were strengthened by implementation of the results of conventional coronary angiography. In all 5 of these patients, conventional coronary angiography confirmed the scintigraphic detection of stenoses of >50%, and interventional therapy was performed. In any event, the preliminary results of this retrospective analysis have to be considered carefully, because it compared an anatomic imaging procedure with a functional imaging procedure. Furthermore, only a small number of patients could be included. Because the use of MDCT angiography is not routine for clinical diagnostics in CAD, we could consider only investigations that had been performed by chance.

CONCLUSION

The positive predictive value of MDCT angiography was weak, at 29%, for detecting areas of ischemia in need of revascularization in a nonselected study cohort. Thus, MPI remains mandatory for evaluating the functional relevance of coronary artery lesions, but the addition of MDCT angiography contributes important morphologic information. Further studies are needed to confirm these preliminary results and to evaluate the ability of combined MDCT angiography and MPI to improve both diagnosis and risk stratification in patients with suspected or known CAD.

ACKNOWLEDGMENT

We are grateful for the support and superb technical assistance of the staff of the Departments of Nuclear Medicine and Radiology at the University of Munich.

REFERENCES

1. Wayhs R, Zelinger A, Raggi P. High coronary artery calcium scores pose an extremely elevated risk for hard events. *J Am Coll Cardiol.* 2002;39:225–230.
2. Detrano RC, Doherty TM, Davies MJ, Stary HC. Predicting coronary events with coronary calcium: pathophysiologic and clinical problems. *Curr Probl Cardiol.* 2000;25:374–402.
3. O'Malley PG, Feuerstein IM, Taylor AJ. Impact of electron beam tomography, with or without case management, on motivation, behavioral change, and cardiovascular risk profile: a randomized controlled trial. *JAMA.* 2003;289:2215–2223.
4. Virmani R, Burke A, Farb A. Coronary risk factors and plaque morphology in men with coronary disease who died suddenly. *Eur Heart J.* 1998;19:678–680.
5. Virmani R, Burke AP, Kolodgie FD, Farb A. Vulnerable plaque: the pathology of unstable coronary lesions. *J Interv Cardiol.* 2002;15:439–446.
6. Virmani R, Kolodgie FD, Burke AP, Farb A, Schwartz SM. Lessons from sudden coronary death: a comprehensive morphological classification scheme for atherosclerotic lesions. *Arterioscler Thromb Vasc Biol.* 2000;20:1262–1275.
7. Kragel AH, Reddy SG, Wittes JT, Roberts WC. Morphometric analysis of the composition of atherosclerotic plaques in the four major epicardial coronary

arteries in acute myocardial infarction and in sudden coronary death. *Circulation.* 1989;80:1747–1756.
8. Kolodgie FD, Burke AP, Farb A, et al. The thin-cap fibroatheroma: a type of vulnerable plaque—the major precursor lesion to acute coronary syndromes. *Curr Opin Cardiol.* 2001;16:285–292.
9. Leber AW, Knez A, White CW, et al. Composition of coronary atherosclerotic plaques in patients with acute myocardial infarction and stable angina pectoris determined by contrast-enhanced multislice computed tomography. *Am J Cardiol.* 2003;91:714–718.
10. Nikolaou K, Sagmeister S, Knez A, et al. Multidetector-row computed tomography of the coronary arteries: predictive value and quantitative assessment of non-calcified vessel-wall changes. *Eur Radiol.* 2003;13:2505–2512.
11. Schroeder S, Kopp AF, Ohnesorge B, et al. Accuracy and reliability of quantitative measurements in coronary arteries by multi-slice computed tomography: experimental and initial clinical results. *Clin Radiol.* 2001;56:466–474.
12. Schroeder S, Kopp AF, Baumbach A, et al. Non-invasive characterisation of coronary lesion morphology by multi-slice computed tomography: a promising new technology for risk stratification of patients with coronary artery disease. *Heart.* 2001;85:576–578.
13. Leber AW, Knez A, Becker A, et al. Accuracy of multidetector spiral computed tomography in identifying and differentiating the composition of coronary atherosclerotic plaques: a comparative study with intracoronary ultrasound. *J Am Coll Cardiol.* 2004;43:1241–1247.
14. Ropers D, Baum U, Pohle K, et al. Detection of coronary artery stenoses with thin-slice multi-detector row spiral computed tomography and multiplanar reconstruction. *Circulation.* 2003;107:664–666.
15. Nieman K, Cademartiri F, Lemos PA, Raaijmakers R, Pattynama PM, de Feyter PJ. Reliable noninvasive coronary angiography with fast submillimeter multislice spiral computed tomography. *Circulation.* 2002;106:2051–2054.
16. Kopp AF, Schroeder S, Kuettner A, et al. Non-invasive coronary angiography with high resolution multidetector-row computed tomography: results in 102 patients. *Eur Heart J.* 2002;23:1714–1725.
17. Knez A, Becker CR, Leber A, et al. Usefulness of multislice spiral computed tomography angiography for determination of coronary artery stenoses. *Am J Cardiol.* 2001;88:1191–1194.
18. Achenbach S, Ulzheimer S, Baum U, et al. Noninvasive coronary angiography by retrospectively ECG-gated multislice spiral CT. *Circulation.* 2000;102:2823–2828.
19. Achenbach S, Daniel WG, Ulzheimer S, et al. Noninvasive coronary angiography: an acceptable alternative? *N Engl J Med.* 2001;345:1909–1910.
20. Kuettner A, Trabold T, Schroeder S, et al. Noninvasive detection of coronary lesions using 16-detector multislice spiral computed tomography technology: initial clinical results. *J Am Coll Cardiol.* 2004;44:1230–1237.
21. Iskander S, Iskandrian AE. Risk assessment using single-photon emission computed tomographic technetium-99m sestamibi imaging. *J Am Coll Cardiol.* 1998; 32:57–62.
22. Gibbons RS. American Society of Nuclear Cardiology project on myocardial perfusion imaging: measuring outcomes in response to emerging guidelines. *J Nucl Cardiol.* 1996;3:436–442.
23. Raiker K, Sinusas AJ, Wackers FJ, Zaret BL. One-year prognosis of patients with normal planar or single-photon emission computed tomographic technetium 99m-labeled sestamibi exercise imaging. *J Nucl Cardiol.* 1994;1:449–456.
24. Brown KA, Altland E, Rowen M. Prognostic value of normal technetium-99m-sestamibi cardiac imaging. *J Nucl Med.* 1994;35:554–557.
25. Pavin D, Delonca J, Siegenthaler M, Doat M, Rutishauser W, Righetti A. Long-term (10 years) prognostic value of a normal thallium-201 myocardial exercise scintigraphy in patients with coronary artery disease documented by angiography. *Eur Heart J.* 1997;18:69–77.
26. Brown KA, Rowen M. Prognostic value of a normal exercise myocardial perfusion imaging study in patients with angiographically significant coronary artery disease. *Am J Cardiol.* 1993;71:865–867.
27. Chamuleau SA, Meuwissen M, van Eck-Smit BL, et al. Fractional flow reserve, absolute and relative coronary blood flow velocity reserve in relation to the results of technetium-99m sestamibi single-photon emission computed tomography in patients with two-vessel coronary artery disease. *J Am Coll Cardiol.* 2001;37:1316–1322.
28. Jakobs TF, Becker CR, Ohnesorge B, et al. Multislice helical CT of the heart with retrospective ECG gating: reduction of radiation exposure by ECG-controlled tube current modulation. *Eur Radiol.* 2002;12:1081–1086.
29. Hong C, Becker CR, Huber A, et al. ECG-gated reconstructed multi-detector row CT coronary angiography: effect of varying trigger delay on image quality. *Radiology.* 2001;220:712–717.
30. Nikolaou K, Knez A, Sagmeister S, et al. Assessment of myocardial infarctions using multidetector-row computed tomography. *J Comput Assist Tomogr.* 2004; 28:286–292.
31. Kuettner A, Kopp AF, Schroeder S, et al. Diagnostic accuracy of multidetector computed tomography coronary angiography in patients with angiographically proven coronary artery disease. *J Am Coll Cardiol.* 2004;43:831–839.
32. Hachamovitch R, Hayes SW, Friedman JD, Cohen I, Berman DS. Comparison of the short-term survival benefit associated with revascularization compared with medical therapy in patients with no prior coronary artery disease undergoing stress myocardial perfusion single photon emission computed tomography. *Circulation.* 2003;107:2900–2907.
33. Wong ND, Vo A, Abrahamson D, Tobis JM, Eisenberg H, Detrano RC. Detection of coronary artery calcium by ultrafast computed tomography and its relation to clinical evidence of coronary artery disease. *Am J Cardiol.* 1994;73:223–227.
34. Berman DS, Wong ND, Gransar H, et al. Relationship between stress-induced myocardial ischemia and atherosclerosis measured by coronary calcium tomography. *J Am Coll Cardiol.* 2004;44:923–930.
35. Pirich C, Leber A, Knez A, et al. Relation of coronary vasoreactivity and coronary calcification in asymptomatic subjects with a family history of premature coronary artery disease. *Eur J Nucl Med Mol Imaging.* 2004;31:663–670.
36. Hachamovitch R, Berman DS, Kiat H, et al. Exercise myocardial perfusion SPECT in patients without known coronary artery disease: incremental prognostic value and use in risk stratification. *Circulation.* 1996;93:905–914.
37. Hachamovitch R, Berman DS, Shaw LJ, et al. Incremental prognostic value of myocardial perfusion single photon emission computed tomography for the prediction of cardiac death: differential stratification for risk of cardiac death and myocardial infarction. *Circulation.* 1998;97:535–543.
38. Christian TF, Miller TD, Bailey KR, Gibbons RJ. Noninvasive identification of severe coronary artery disease using exercise tomographic thallium-201 imaging. *Am J Cardiol.* 1992;70:14–20.
39. Travin MI, Katz MS, Moulton AW, Miele NJ, Sharaf BL, Johnson LL. Accuracy of dipyridamole SPECT imaging in identifying individual coronary stenoses and multivessel disease in women versus men. *J Nucl Cardiol.* 2000;7:213–220.
40. Schindler TH, Magosaki N, Jeserich M, et al. 3D assessment of myocardial perfusion parameter combined with 3D reconstructed coronary artery tree from digital coronary angiograms. *Int J Card Imaging.* 2000;16:1–12.
41. Schindler TH, Magosaki N, Jeserich M, et al. Fusion imaging: combined visualization of 3D reconstructed coronary artery tree and 3D myocardial scintigraphic image in coronary artery disease. *Int J Card Imaging.* 1999;15:357–368.
42. Faber TL, Stokely EM, Templeton GH, Akers MS, Parkey RW, Corbett JR. Quantification of three-dimensional left ventricular segmental wall motion and volumes from gated tomographic radionuclide ventriculograms. *J Nucl Med.* 1989;30:638–649.

JNM The Journal of NUCLEAR MEDICINE

Comparison of Spiral Multidetector CT Angiography and Myocardial Perfusion Imaging in the Noninvasive Detection of Functionally Relevant Coronary Artery Lesions: First Clinical Experiences

Marcus Hacker, Tobias Jakobs, Florian Matthiesen, Christian Vollmar, Konstantin Nikolaou, Christoph Becker, Andreas Knez, Thomas Pfluger, Maximilian Reiser, Klaus Hahn and Reinhold Tiling

J Nucl Med. 2005;46:1294-1300.

The Journal of Nuclear Medicine is published monthly.
SNMMI | Society of Nuclear Medicine and Molecular Imaging
1850 Samuel Morse Drive, Reston, VA 20190.
(Print ISSN: 0161-5505, Online ISSN: 2159-662X)

SNMMI SOCIETY OF NUCLEAR MEDICINE AND MOLECULAR IMAGING